Acta Polytechnica **65**(3):361–370, 2025
https://doi.org/10.14311/AP.2025.65.0361

ANALYSIS OF SURFACE ROUGHNESS AND MACHINING PERFORMANCE OF AZ91 MAGNESIUM ALLOY CUT BY WEDM

Levent Urtekin[a], Faik Yilan[a,*], İbrahim Baki Şahin[a], Kadir Gök[b]

[a] *Kırşehir Ahi Evran University, Faculty of Engineering and Architecture, Department of Mechanical Engineering, 40100 Kırşehir, Turkey*

[b] *İzmir Bakırçay University, Engineering and Architecture Faculty, Department of Biomedical Engineering, 35660 İzmir, Turkey*

[*] corresponding author: faik.yilan@ahievran.edu.tr

Abstract. AZ91 magnesium alloys have poor machinability when conventional chip removal processes are used due to their low thermal stability and high susceptibility to softening and oxidation at elevated temperatures, which lead to excessive tool wear, poor surface quality, and deformation-induced machining challenges. This study investigated the impact of wire electrical discharge machining (WEDM) parameters on material removal rate (MRR) and surface roughness (SR) using magnesium. For this purpose, an analysis of variance (ANOVA) and Grey Relational Analysis (GRA) were performed to find the optimal settings. Findings indicate that pulse-on time (T_{on}) significantly affects both MRR and SR: higher T_{on} increases MRR but worsens SR, while shorter T_{on} improves SR but reduces MRR. Pulse-off time (T_{off}) and wire feed rate (WF) have secondary effects. Longer T_{off} improves surface quality but slightly reduces MRR, and lower WF improves cutting efficiency and MRR. The optimal settings identified by the Taguchi method were observed to be 123 µs T_{on}, 55 µs T_{off}, and 6 m min^{-1} WF for high MRR; and 123 µs T_{on}, 58 µs T_{off}, and 4 m min^{-1} WF for reduced SR. In summary, understanding how WEDM parameters affect MRR and SR allows manufacturers to achieve efficient material removal and desired surface quality.

Keywords: AZ91, WEDM, material removal rate (MRR), surface roughness (SR), optimisation.

1. Introduction

Biomaterials such as implants, plates, and screws used in orthopaedic and dental surgeries must be chosen carefully for stabilisation and fracture healing. The biomechanical behaviour of these materials affects stability and implant failure can lead to repeated surgeries, increasing risks for older patients [1–4]. In 2019, there were 178 million new fractures globally, with 455 million cases of fracture symptoms, including 25.8 million years lived with disability [5]. Successful fracture management is crucial, with fixation materials playing a key role. Studies have examined implant design, materials, and fatigue behaviour. Sykaras et al. [6] reviewed dental implant materials and designs, while other studies used three-dimensional analyses and finite element models for hip implants [7].

Third-generation biomaterials such as magnesium alloys are increasingly used in orthopaedic applications due to their unique properties, including high biocompatibility, good biodegradability, and satisfactory mechanical properties [8–10]. The most popular magnesium alloy is AZ91, which has a high strength-to-weight ratio, reduced castability, and resistance to corrosion. Due to the low yield strength of AZ91 magnesium alloy, it is recommended for use in situations with minimal movement or low loads. However, its mechanical properties can be improved through various heat treatments or by adding strength-enhancing alloying elements [11, 12]. According to Kuyubasi et al. [13] the biomechanical behaviour of three different screw materials (Ti_6Al_4V, MgAZ91, and Ti_6Al_4V-HA) was analysed for fixing femoral neck fractures with triangular fixation under axial loading to determine which material performed better biomechanically. The authors believe that the investigated fixation materials could play a role in reducing the need for recurrent anesthesia and orthopaedic surgical risks. Magnesium alloys such as AZ91 have attracted significant attention for their potential as biodegradable implant materials. However, their rapid corrosion rate remains a major drawback, as this can occur faster than bone healing, possibly compromising the mechanical integrity of the implant before the tissue regeneration completes [14, 15] Therefore, further research into the degradation mechanisms of these alloys is required. In addition to magnesium alloys, high-performance biomaterials such as titanium and stainless steel alloys are also widely used for biomedical implants due to their excellent mechanical properties and corrosion resistance.

The applicability of this AZ91 alloy is, however, restricted due to its high processing costs, low workability (because of its hexagonal close-packed (HCP) structure), and loss of mechanical qualities at high temperatures. Due to their physical and mechanical characteristics, magnesium alloys are highly machinable by conventional machining processes; however, when it comes to producing complex and 3D intricate shapes with high geometrical accuracy and productivity, or reaching the desired dimension with the least amount of material elimination, traditional machining processes fall short in terms of efficiency and precision. As a result, non-traditional machining methods need be developed [16, 17].

In WEDM processes, choosing the best machining parameters results in higher productivity and well-functioning machined components [18, 19]. WEDM, the most widely used unconventional machining technique, removes material from the workpiece to create objects with intricate profiles and shapes. This process removes the material from the workpiece by creating a sequence of discrete spark discharges between the tool and the work electrode that are dipped in a liquid dielectric medium. A tiny quantity of the work material evaporates when the spark caused by the electrical discharge melts. The removed material is cleared and ejected using the dielectric [20, 21].

Some researchers have examined the performance of the WEDM process on Mg-based alloy materials [22–26]. As clearly understood from these studies, the obtained results depend on the process input parameters according to various factors affecting the machining performance and productivity [27–30]. In addition to preliminary studies, the optimisation of the WEDM process parameters have been performed more recently. Kumar et al. [31] investigated the influence of WEDM process parameters on material removal, surface characteristics, and corrosion rate of ZE41A Mg alloy. The research used a Taguchi L16 orthogonal array to measure the corrosion rate (CR) after a week of immersion in simulated body fluid. GRA was used to simultaneously optimise MRR, SR, and CR. Also, the studies indicated that optimum WEDM parameters improved performance, reduced SR, and reduced in-vitro CR, thereby mitigating mechanical integrity loss in bone design. In another study, Goyal et al. [32] used WEDM to process AZ31 alloy, focusing on input machining variables and response characteristics. The variables include servo feed, voltage, T_{on}, and T_{off}. ANOVA analyses was used to analyse each response, and empirical models were used to identify Pareto fronts in the various process. The multi objective grey wolf optimisation algorithm (MOGWO) was improved using the Levy flight algorithm. The improved MOGWO efficiently detected uniformly distributed Pareto fronts. Results were validated through confirmation experiments and the morphology was evaluated using scanning electron microscopy (SEM) to identify microcracks, globules, micropores, and lumps. Similarly, Muniappan et al. [33] investigated the impact of machining control parameters on kerf width (KW) and cutting speed (CS) in WEDM processes. Multi objective optimisation by ratio analysis (MOORA) can be achieved to optimise kerf width and cutting speed. The study found that T_{on}, T_{off}, peak pulse current, gap voltage, WF, and wire tension were the best combinations for improving CS and KW. Gotagunaki et al. [34] also investigated optimal values of the WEDM process parameters for milling AZ91D magnesium alloy using response surface methodology (RSM) and ANOVA. Surface flaws such as globules, recast layers, holes, and surface voids were identified on the machined material at higher cutting speeds. The ANOVA data indicate that the T_{on} is the most significant variable, with peak current being the second.

According to the literature, machining parameters are crucial in determining the SR and MRR of WEDM processing. However, limited research has been carried out on the processing of AZ91 alloys. Therefore, the aim of this study is to investigate the effects of pulse on time, pulse off time, and wire feed speed as well as processing input parameters on the machining performance of AZ91 alloys. The obtained MRR and SR values were optimised. Thus, the usability of these processes will be determined by optimising the parameters of the tested processes of AZ91 alloy, one of the most widely used metallic biomaterials in biomedical applications.

2. Experimental design

2.1. Materials

The material chosen for this study is AZ91 magnesium (Mg) alloy, one of the most widely and successfully used commercial alloys among magnesium-based materials, owing to its excellent combination of mechanical properties, lightweight characteristics, and corrosion resistance. Table 1 provides information on MgAZ91.

The microstructure of the MgAZ91 alloy observed post-casting, as depicted in Figure 1, reveals a matrix composed primarily of α-Mg, along with a network of intermetallic phases, likely identified as γ. Additionally, non-equilibrium eutectic structures are evident in the vicinity of these intermetallic precipitates. Such microstructural inhomogeneities result in non-uniform deformation during mechanical loading. Furthermore, these hard intermetallic phases and precipitates can act as stress concentration sites, increasing the likelihood of crack initiation and propagation.

3. Taguchi experimental design

The Design of Experiment (DOE) is a crucial methodology used in experimental research to generate data that are statistically robust and analysable. It is a key tool for determining the best conditions while reducing the number of experiments needed. Within the various experimental design techniques available, the Taguchi method is particularly notable for its structured approach. This method begins with defining the response variable or objective function that needs to be studied. It then involves identifying the factors that affect this response variable. The next step is to set different levels for these factors. This is followed by

Element	Mg	Al	Zn	Mn	Cu	Ni
Content [%]	89.52	8.50	0.45	0.17	0.03	0.002

TABLE 1. The chemical composition of AZ91.

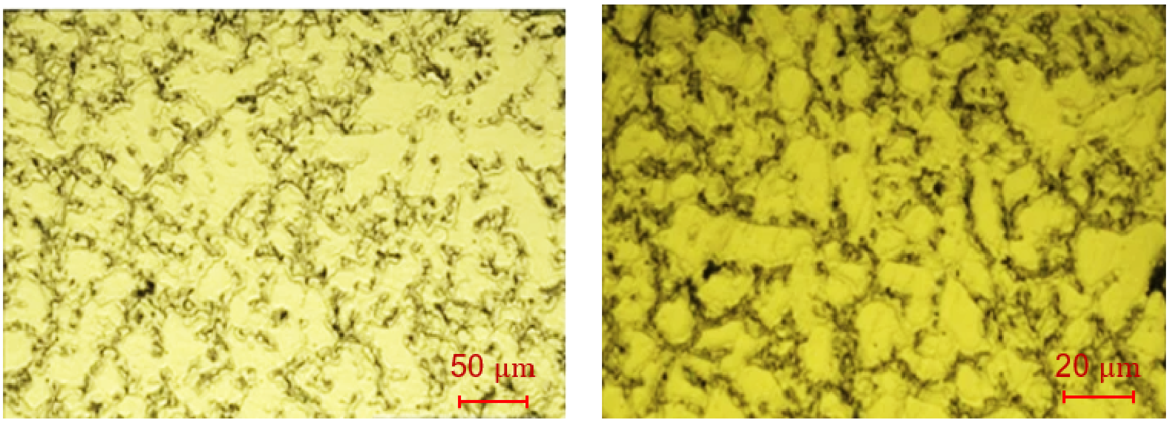

(A). Optical micrograph of etched AZ91 Mg alloy.

(B). Scanning electron microscope (SEM) micrograph of the etched AZ91 Mg alloy sample.

FIGURE 1. Optical microscope image of the MgAZ91 alloy.

	Units	Levels 1	2	3
Pulse on time (T_{on})	µs	110	117	123
Pulse off time (T_{off})	µs	55	58	62
Wire feed rate (WF)	$\text{mm}\,\text{min}^{-1}$	4	6	-

TABLE 2. The variable parameters and levels used for the DOE.

conducting experiments using an orthogonal array to evaluate the impact of these factor levels, as noted in references [35]. The final step in this process is to pinpoint the optimal levels of these factors to improve the response variable. The Taguchi robust parameter design method is well-regarded for its utility in designing experiments and optimising processes, often used to improve quality control measures offline, as discussed in literature [36–38]. The parameters and levels of parameters are presented in Table 2. The signal-to-noise ratio ($\frac{S}{N}$ ratio), used as one of the performance functions in the Taguchi method, is generally divided into three main categories: smaller-the-better, larger-the-better, and nominal-the-best. In this study, the larger-the-better characteristic is used for the MRR response, while the smaller-the-better characteristic is used for the (SR) response. The MRR and SR are obtained using Equations (1) and (2).

$\frac{S}{N}$ ratio for larger-the-better characteristic:

$$\frac{S}{N}\ \text{ratio}(\eta) = -10\log_{10}\left(\frac{1}{n}\sum_{i=1}^{n}\frac{1}{y_{ij}^2}\right), \tag{1}$$

$\frac{S}{N}$ ratio for smaller-the-better characteristic:

$$\frac{S}{N}\ \text{ratio}(\eta) = -10\log_{10}\left(\frac{1}{n}\sum_{i=1}^{n}y_{ij}^2\right), \tag{2}$$

where n corresponds to the number of experiments and y_{ij} refers to the response value for the corresponding experiments [39–41].

A key feature of the Taguchi method is the use of specially crafted orthogonal arrays that allow for a comprehensive analysis of all the parameters involved with fewer experiments. These arrays are organised in a matrix format where rows represent the experiments and columns represent the factors affecting the response variable, as detailed in sources [42, 43]. This setup allows the determination of the best parameter levels for the desired outcome. For example, a Taguchi L36 orthogonal array, which includes three levels for two factors, was used in the experimental framework outlined in Table 3. The choice of factors and their levels was influenced by previous research findings. The ANOVA output comprises several statistical parameters, including the degree of freedom (DF), Fischer's F distribution (F-value), sources of variation (control factors, error, and the total of all sources), adjusted mean squares (Adj MS), P-value, adjusted sum of squares (Adj SS), and the percentage contribution of the control factors. The statistical significance of the results is determined based on the P-value; specifically, a P-value below 0.05 indicates that the corresponding control factor has a statistically significant influence on the response param-

# run	T_{on} [μs]	T_{off} [μs]	WF [mm min^{-1}]
1.	110	62	4
2.	110	58	4
3.	110	55	4
4.	110	62	4
5.	110	58	4
6.	110	55	4
7.	110	62	6
8.	110	58	6
9.	110	55	6
10.	110	62	6
11.	110	58	6
12.	110	55	6
13.	117	62	4
14.	117	58	4
15.	117	55	4
16.	117	62	4
17.	117	58	4
18.	117	55	4
19.	117	62	6
20.	117	58	6
21.	117	55	6
22.	117	62	6
23.	117	58	6
24.	117	55	6
25.	123	62	4
26.	123	58	4
27.	123	55	4
28.	123	62	4
29.	123	58	4
30.	123	55	4
31.	123	62	6
32.	123	58	6
33.	123	55	6
34.	123	62	6
35.	123	58	6
36.	123	55	6

Table 3. L36 Taguchi orthogonal array for the DOE.

eter [44]. The percentage contribution reflects the extent to which a particular control factor impacts the response parameter, offering insight into its relative importance. Furthermore, within the ANOVA model, S represents the standard deviation of the observed data and fitted values, R-sq denotes the proportion of variance in the response variable explained by the model, and R-sq (adj) provides a modified version of R-sq by considering the number of predictors relative to the number of observations, thereby preventing overfitting. Equations (3)–(6) are used to derive the key indicators of the ANOVA method, which include the degrees of freedom (DF), sum of squares (SS), mean squares (MS), F-values, and contribution ratio (CR) for each factor. These parameters serve as the fundamental components for assessing the influence and statistical significance of individual factors on the response variable, providing a comprehensive quantitative analysis of the experimental data [40].

$$\mathrm{DF} = \sum_{i=1}^{n_f} (L_i - 1) + \mathrm{DF}_{\mathrm{error}}, \tag{3}$$

where L_i is the number of levels, n_f is the number of factors, and $\mathrm{DF}_{\mathrm{error}}$ is the degree of freedom for the error.

$$\mathrm{SS}_i = \sum_{i=1}^{n} (\hat{y}_i - \bar{y})^2, \tag{4}$$

where, $\bar{y}$ is the mean response value, $\hat{y}_i$ is the i^{th} response value.

The corresponding means of squares are given by:

$$\mathrm{MS}_i = \frac{\mathrm{SS}_i}{\mathrm{DF}_i}. \tag{5}$$

The F-factor, which reflects the statistical reliability of the results, is given by the ratio of the parameter's mean square to the mean square error:

$$F_i = \frac{\mathrm{MS}_i}{\mathrm{MS}_{\mathrm{error}}}. \tag{6}$$

The contribution ratio (CR) is defined as the ratio of the sum of squared deviations to the total sum of squared deviations [45]:

$$\%\ \mathrm{Contribution}_i = \frac{\mathrm{SS}_i}{\mathrm{SS}_T}. \tag{7}$$

3.1. Analysis and characterisation of the samples

The surface images and the chemical element analysis of the samples were analysed and characterised using a Hitachi Regulus 8230 scanning electron microscope (SEM). The microstructures were examined by optical microscopy. The ZeGage optical profiler instrument was used to measure the average SR data. The surface roughness (SR) was measured perpendicular to the tool path following the ISO 1997 standard, with a sample length of 4 mm. The SR of the specimen was recorded as the average value obtained from three measurements.

4. WEDM experimental setup

The dimensions of the MgAZ91 workpiece used in this study are 200 mm × 200 mm × 5 mm; however, the specimen size that was removed from it is 10 mm × 10 mm × 5 mm. Ultracut F1, ELPULS 501 WEDM machine was used in this study. Using an electrode made of 250 μm-diameter brass wire, the workpiece of AZ91 Mg alloy (flat plate) was machined. Maximum machining current was recorded during the sample's WEDM process when the wire had reached the sample's full diameter. This number was recorded and used in the experiments. Throughout the studies, a wire tension of 8 N was applied. To flush the dirt

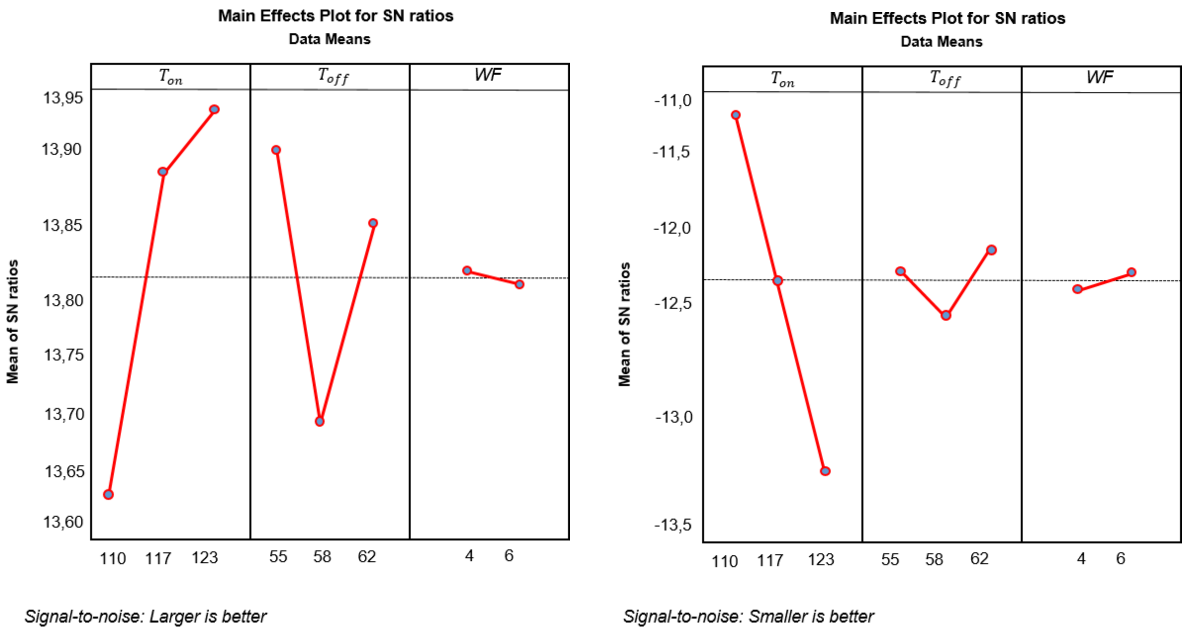

(a). MRR. (b). SR.

Figure 2. MRR and SR for the $\frac{S}{N}$ graphs.

Source	DF	Adj SS	Adj MS	*F*-Value	*P*-Value	Contribution %
T_{on}	2	0.16722	0.083611	3.14	0.058	15.841828
T_{off}	2	0.09056	0.045278	1.7	0.199	8.5793323
WF	1	0	0	0	1	0
Error	30	0.79778	0.026593			75.57884
Total	35	1.05556				100

Table 4. ANOVA analysis results for MRR.

out of the gap between the wire and the workpiece, distilled water was used as a dielectric fluid. The differences in the machining performance outputs (MRR and SR) were examined in order to modify the WEDM parameters (T_{on}, T_{off} and WF) for the samples.

5. Results and discussions

5.1. WEDM machining factors optimisation

5.1.1. ANOVA analysis of MRR and SR

The main effects plot of the mean MRR and SR is presented in Figure 2. The ANOVA method is used to analyse experimental data and assess the impact of different parameters. It is a statistical tool that helps identify differences in the average performance of different groups of parts. ANOVA enables the determination of which parts are suitable for specific processes and their respective performance levels. The analysis of variance aims to assess the extent to which the elements being studied progress, the quality of the output values chosen for measurement, and the various levels that cause variations [46].

In the analysis of ANOVA results for MRR in MgAZ91 WEDM, as presented in Table 4, it is observed that the T_{on} significantly influences the MRR, accounting for 15.8 % of the variance. This significant impact can be attributed to the fact that longer pulse-on times allow for more energy to be discharged between the wire and the workpiece, thereby enhancing the material removal rate. Similarly, the T_{off} contributes to 8.57 % of the variance in MRR. The pulse-off time is crucial as it allows the spark to cool down and debris to be flushed away, thus preventing excessive tool wear and workpiece damage, which can affect the efficiency of the machining process. However, the wire speed shows no significant effect on the MRR. This could be due to the specific properties of magnesium and the settings of the WEDM process used in this study, where variations in wire speed do not significantly alter the dynamics between the electrode wire and the magnesium workpiece, thus having a minimal impact on the rate of material removal. In the machining of AZ91 magnesium alloy, it was observed that both the MRR and WF were higher compared to other materials. Specifically, the MRR reached 180 $mm^3\,min^{-1}$, while the WF measured 0.450 mm. The primary factors contributing to this behaviour are the low melting point and high thermal conductivity of magnesium alloys. These characteristics facilitate easier material removal due to reduced cutting resistance and promote efficient thermal dissipation during

Source	DF	Adj SS	Adj MS	*F*-Value	*P*-Value	Contribution %
T_{on}	2	6.5646	3.28203	35.22	0	68.526455
T_{off}	2	0.2172	0.10851	1.16	0.326	2.2656117
WF	1	0.0025	0.00251	0.03	0.871	0.0262035
Error	30	2.7952	0.09318			29.18173
Total	35	9.5788				100

TABLE 5. ANOVA analysis results for SR.

the machining process, which in turn affects the kerf dimensions [28]. An increase in pulse-off time leads to a reduction in the number of sparks generated per unit of time. Consequently, the energy available for material removal decreases. As a result, the MRR decreases, although the reduction occurs with relatively small incremental changes in pulse-off time. This behaviour contrasts with the effect of increasing pulse-on time, which typically results in a higher MRR due to the greater energy input during each spark [34].

In the analysis of ANOVA results for surface roughness of MgAZ91 WEDM, as presented in the Table 5, it is evident that the T_{on} has a substantial impact on surface roughness, accounting for 68.25 % of the variance. This pronounced effect is likely because longer pulse-on times increases the amount of energy discharged between the wire and the workpiece, which can lead to larger and deeper craters on the surface, thereby increasing roughness. Conversely, the T_{off} shows a relatively minor contribution, having only 2.2 % of the variance in surface roughness. The smaller influence of T_{off} on the surface roughness suggests that the cooling and debris flushing intervals, while essential for maintaining the integrity of the cut and preventing wire breakage, have a less direct effect on the textural quality of the surface. This analysis highlights the dominant role of T_{on} in determining the quality of the surface finish in WEDM processes, emphasising the need for careful setting of pulse durations to optimise surface characteristics.. Despite the high cutting rates observed during the WEDM of MgAZ91 alloys, the SR values remained within acceptable limits, highlighting the excellent machinability of these materials. The maximum recorded SR value was 4.683 µm, demonstrating that even at high material removal rates, the process produced surfaces of sufficient quality, further emphasising the suitability of MgAZ91 for precision machining applications [28]. During the investigation, it was found that pulse-on time has the major influence on surface roughness while voltage and pulse-off time have a lesser influence on the surface roughness.

The optimal parameters have been identified by examining the Signal-to-Noise ($\frac{S}{N}$) ratio graphs for WEDM based on their effects on MRR and SR. For maximising MRR, the optimal settings are found to be $T_{on} = 123$ microseconds, $T_{off} = 55$ microseconds, and a WF rate of 6 metres per minute. These settings likely provide a balance between efficient material removal and maintaining operational stability, allowing for a higher discharge energy that improves the cutting efficiency without excessive tool wear or damage. When focusing on minimising SR, the optimal parameters slightly differ. The best results are achieved with $T_{on} = 123$ microseconds, similar to the MRR settings, which suggests that this pulse duration effectively controls the energy input to both maximise the removal rates and manage the surface finish. However, the T_{off} is slightly increased to 58 microseconds, and the WF rate is reduced to 4 metres per minute. The increased T_{off} allows more time for debris expulsion and cooling, which helps in achieving a smoother surface by reducing the thermal impact on the workpiece. The reduced wire feed rate decreases the interaction time between the wire and the workpiece, potentially leading to finer surface finishes. These findings illustrate the importance of precisely adjusting the WEDM parameters to optimise different aspects of the machining process, depending on the specific machining outcomes desired.

The surface plots showing the effects of T_{on}, T_{off}, and WF on MRR and SR are shown in Figure 3. The x and y-axes represent the machining parameters (T_{on} and T_{off}), while the z-axis denotes the response variables (MRR in $mm^3 min^{-1}$ and SR in µm). A gradient colour scheme on the z-axis highlights the minima and maxima of the response values, aiding in the identification of optimal parameter combinations for WEDM. As depicted in Figure 3, distinct relationships between machine settings and machining outcomes are observed in the exploration of parameter effects in WEDM, specifically concerning MRR and SR. The analysis reveals a positive correlation between T_{on} and MRR. As T_{on} increases, more energy is delivered to the workpiece, facilitating improved material removal rate. This relationship underscores the importance of T_{on} in optimising the efficiency of the WEDM process. Additionally, the data indicates that decreasing both the WF rate and the T_{off} contributes to an increase in MRR. A lower WF rate likely aids in maintaining the structural integrity of the wire, thus ensuring consistent cutting conditions, while a reduced T_{off} minimises idle time between discharges, maximising the material removal rate.

Conversely, the study of SR demonstrates that increases in both T_{on} and T_{off} are associated with deteriorated surface finishes. An extended T_{on} leads to larger energy discharges, which create deeper and more pronounced craters on the workpiece surface,

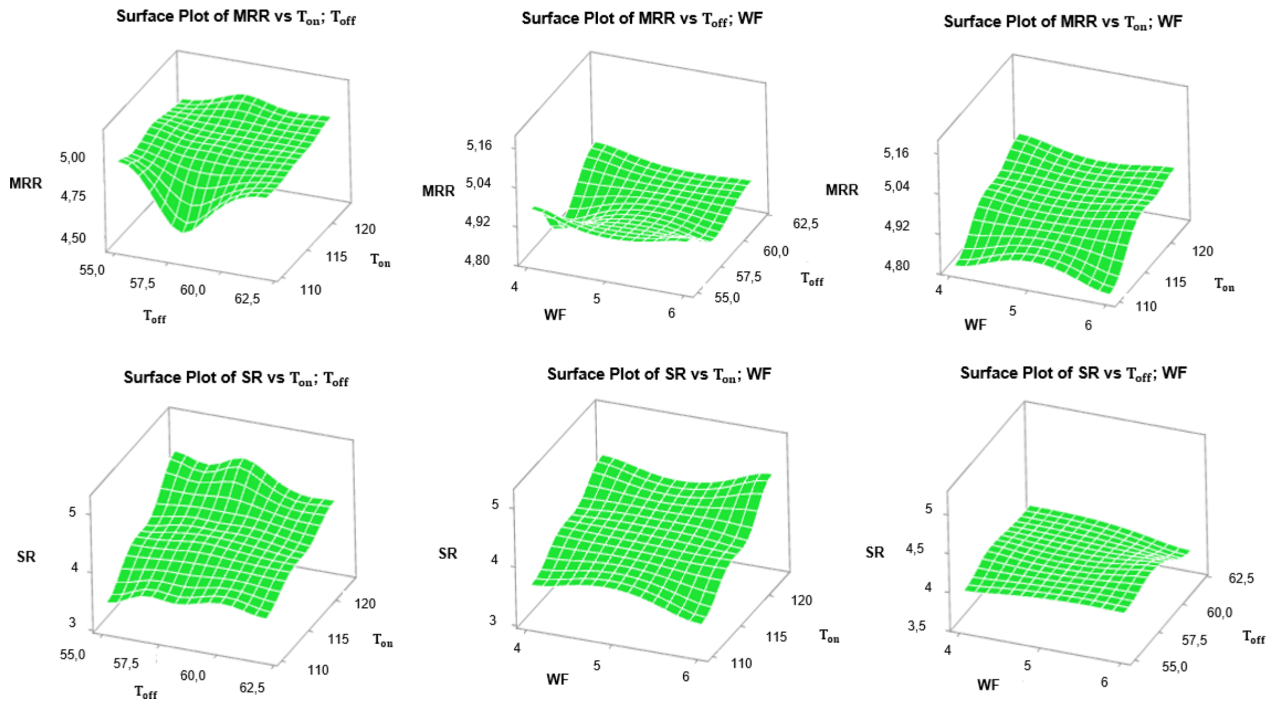

FIGURE 3. Surface plot for MRR and SR.

thereby increasing roughness. Furthermore, a longer T_{off} allows the molten debris more time to resettle on the workpiece in an uneven manner before the next discharge, exacerbating the roughness of the finished surface. These insights highlight the nuanced trade-offs between increasing MRR and minimising SR in WEDM. The findings from Figure 3 provide a comprehensive understanding of how WEDM parameters must be meticulously managed to achieve the desired machining performance, emphasising the need for strategic parameter optimisation based on specific production goals.

5.1.2. Grey Relational Grade analysis

Table 6 presents the outcomes of the Grey Relational Grade (GRG) analysis conducted on 36 distinct cases. The GRG values span from a minimum of 0.5062 to a maximum of 1.0000, demonstrating considerable variability in relational performance among the cases. The highest GRG value of 1.0000 signifies an optimal relationship, indicating that the corresponding case exhibits the most favourable performance within the dataset. Conversely, the lowest GRG value of 0.5062 reflects a weaker relational performance, highlighting potential areas for improvement. The distribution of GRG values across the dataset shows significant concentrations in the mid to upper ranges, suggesting that many cases exhibit moderate to high relational performance. This table offers a detailed overview of the relational efficiencies across the analysed cases, providing a crucial reference point for subsequent comparisons and analytical evaluations.

No.	GRG	No.	GRG	No.	GRG
1.	1.0000	13.	0.8693	25.	0.7680
2.	0.8255	14.	0.7485	26.	0.6526
3.	0.7826	15.	0.7004	27.	0.6156
4.	0.9978	16.	0.8090	28.	0.7915
5.	0.7346	17.	0.6864	29.	0.6235
6.	0.7722	18.	0.6911	30.	0.6495
7.	0.8206	19.	0.7364	31.	0.6222
8.	0.6931	20.	0.6054	32.	0.5108
9.	0.6385	21.	0.5747	33.	0.5080
10.	0.7903	22.	0.7443	34.	0.6703
11.	0.5952	23.	0.5454	35.	0.4530
12.	0.6664	24.	0.5324	36.	0.5062

TABLE 6. GRG analysis results.

6. Surface roughness results

Surface roughness is a paramount consideration in the finished cut of WEDM, impacting both the functional and aesthetic qualities of the machined components. This study aims to elucidate the influence of key machining parameters, which are the pulse-on time, pulse-off time, and wire speed, on surface roughness. A comprehensive understanding of these parameters is essential for optimising WEDM processes to achieve better surface finishes. Furthermore, the single discharge studies revealed that once the pulse energy was lowered to a specific value, craters on the workpiece surface could no longer be produced by a long pulse duration with a low peak value. Even yet, there is still a chance that the workpiece surface will have noticeable craters due to the short pulse length and high peak value. This suggests that longer pulses are

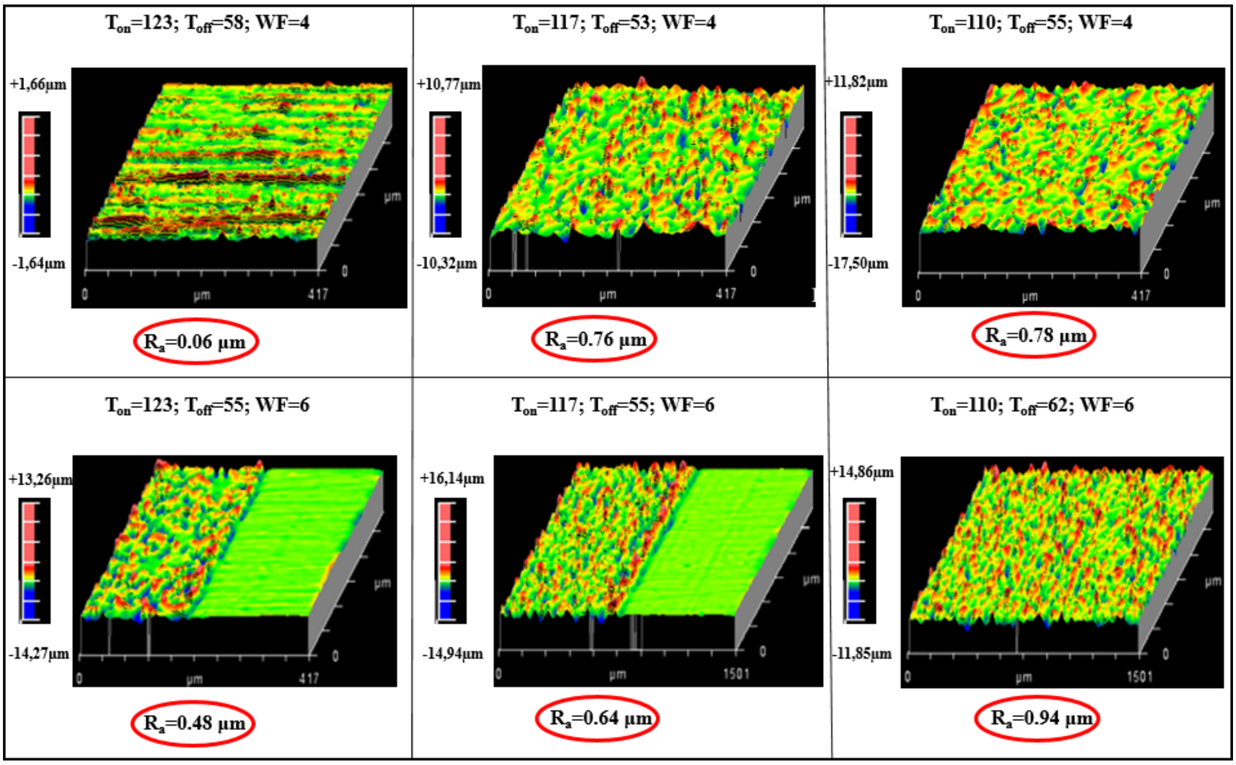

Figure 4. Surface topography maps of samples depending on WEDM process parameters.

unable to produce the same level of surface roughness as short pulses combined with high peak values. Roughness maps of the samples are shown in Figure 4. Higher pulse-on times produce better roughness metric SR. When comparing the surface roughness values of the samples, it is observed that the sample with $T_{\text{on}} = 123$, $T_{\text{off}} = 58$, and WF $= 4$ exhibits the best surface quality. In contrast, the surface roughness values increase for the samples with $T_{\text{on}} = 110$, $T_{\text{off}} = 55$, and WF $= 4$ and $T_{\text{on}} = 110$, $T_{\text{off}} = 62$, and WF $= 6$. The lower surface roughness values of the sample with $T_{\text{on}} = 123$, $T_{\text{off}} = 58$, and WF $= 4$ are attributed to the reduction in heat intensity and the duration of heat application to the workpiece as the WEDM pulse on time increases. Consequently, it can be concluded that the number of pulsed sparks per unit area of the surface not only decreases but also prevents the formation of deep craters.

7. Conclusion

The present work involved a detailed investigation analysed the effects of WEDM parameters on the MRR and SR for MgAZ91 magnesium alloy, and the following conclusions were made as a result of the investigation of its machining properties:

- T_{on} is the most critical factor for both the MRR and SR. Increasing T_{on} increases MRR but worsens surface quality, while a shorter T_{on} improves surface quality but decreases MRR.
- T_{off} has a secondary effect. A longer T_{off} improves surface smoothness, but slightly reduces MRR.
- WF also affects MRR; a lower WF improves wire integrity and cutting efficiency, increasing MRR.
- The Taguchi method identified the following settings as optimal for high MRR; $T_{\text{on}} = 123\,\mu\text{s}$, $T_{\text{off}} = 55\,\mu\text{s}$, and WF $= 6\,\text{m}\,\text{min}^{-1}$. For reduced surface quality, the optimal settings were found to be: $T_{\text{on}} = 123\,\mu\text{s}$, $T_{\text{off}} = 58\,\mu\text{s}$, and WF $= 4\,\text{m}\,\text{min}^{-1}$.

These findings underscore the importance of selecting the optimal WEDM parameters to balance the MRR and SR based on the machining needs. In conclusion, this research offers valuable insights into optimising WEDM processes for magnesium, allowing efficient material removal while maintaining the desired surface quality.

References

[1] W. Pignaton, J. R. C. Braz, P. S. Kusano, et al. Perioperative and anesthesia-related mortality: An 8-year observational survey from a tertiary teaching hospital. *Medicine (Baltimore)* **95**(2):e2208, 2016. https://doi.org/10.1097/MD.0000000000002208

[2] B. F. N. Pascal, A. Malisawa, A. Barratt-Due, et al. General anaesthesia related mortality in a limited resource settings region: A retrospective study in two teaching hospitals of Butembo. *BMC Anesthesiology* **21**(1):60, 2021. https://doi.org/10.1186/s12871-021-01280-2

[3] M. S. Çömez, H. Demirkıran. Intraoperative anesthesia-related mortality: A 10-year survey in a tertiary teaching hospital. *Van Medical Journal* **28**(2):280–287, 2021. https://doi.org/10.5505/vtd.2021.02259

[4] Q. Chen, G. A. Thouas. Metallic implant biomaterials. *Materials Science and Engineering: R: Reports* **87**:1–57, 2015. https://doi.org/10.1016/j.mser.2014.10.001

[5] A.-M. Wu, C. Bisignano, S. L. James, et al. Global, regional, and national burden of bone fractures in 204 countries and territories, 1990–2019: A systematic analysis from the Global Burden of Disease Study 2019. *The Lancet Healthy Longevity* **2**(9):E580–E592, 2021. https://doi.org/10.1016/S2666-7568(21)00172-0

[6] N. Sykaras, A. M. Iacopino, V. A. Marker, et al. Implant materials, designs, and surface topographies: Their effect on osseointegration. A literature review. *International Journal of Oral & Maxillofacial Implants* **15**(5):675–690, 2000.

[7] V. Waide, L. Cristofolini, J. Stolk, et al. Modelling the fibrous tissue layer in cemented hip replacements: Experimental and finite element methods. *Journal of Biomechanics* **37**(1):13–26, 2004. https://doi.org/10.1016/S0021-9290(03)00258-6

[8] K. Kumar, R. S. Gill, U. Batra. Challenges and opportunities for biodegradable magnesium alloy implants. *Materials Technology* **33**(2):153–172, 2017. https://doi.org/10.1080/10667857.2017.1377973

[9] G. E. J. Poinern, S. Brundavanam, D. Fawcett. Biomedical magnesium alloys: A review of material properties, surface modifications and potential as a biodegradable orthopaedic implant. *American Journal of Biomedical Engineering* **2**(6):218–240, 2012. https://doi.org/10.5923/j.ajbe.20120206.02

[10] Y. F. Zheng, X. Gu, F. Witte. Biodegradable metals. *Materials Science and Engineering: R: Reports* **77**:1–34, 2014. https://doi.org/10.1016/j.mser.2014.01.001

[11] K. Majerski, E. Siemionek, M. Szucki, P. Surdacki. Investigations of the effect of heat treatment and plastic deformation parameters on the formability and microstructure of AZ91 alloy castings. *Advances in Science and Technology Research Journal* **18**(1):1–9, 2024. https://doi.org/10.12913/22998624/174932

[12] E. Jonda, L. Łatka, A. Lont, et al. The effect of HVOF spray distance on solid particle erosion resistance of WC-based cermets bonded by Co, Co-Cr and Ni deposited on Mg-alloy substrate. *Advances in Science and Technology Research Journal* **18**(2):115–128, 2024. https://doi.org/10.12913/22998624/184025

[13] A. Gok, L. Urtekin, K. Gok, et al. Computer aided analysis of biomechanical performance of schanz screw with different additive manufacturing materials used in pertrochanteric fixator on an intertrochanteric femoral fracture (corrosion resistance approach). *International Journal for Numerical Methods in Biomedical Engineering* **39**(12):e3763, 2023. https://doi.org/10.1002/cnm.3763

[14] B. Barani, A. K. Lakshminarayanan, R. Subashini, et al. Microstructural characteristics of chitosan deposited AZ91. *Materials Today: Proceedings* **16**:456–462, 2019. https://doi.org/10.1016/j.matpr.2019.05.115

[15] D. Bairagi, S. Mandal. A comprehensive review on biocompatible Mg-based alloys as temporary orthopaedic implants: Current status, challenges, and future prospects. *Journal of Magnesium and Alloys* **10**(3):627–669, 2022. https://doi.org/10.1016/j.jma.2021.09.005

[16] F. Klocke, M. Schwade, A. Klink, A. Kopp. EDM machining capabilities of magnesium (Mg) alloy WE43 for medical applications. *Procedia Engineering* **19**:190–195, 2011. https://doi.org/10.1016/j.proeng.2011.11.100

[17] J. Xu, K. Xia, Z. Lian, et al. Surface properties on magnesium alloy and corrosion behaviour based high-speed wire electrical discharge machine power tubes. *Micro & Nano Letters* **11**(1):15–19, 2016. https://doi.org/10.1049/mnl.2015.0204

[18] K. H. Ho, S. T. Newman, S. Rahimifard, R. D. Allen. State of the art in wire electrical discharge machining (WEDM). *International Journal of Machine Tools and Manufacture* **44**(12–13):1247–1259, 2004. https://doi.org/10.1016/j.ijmachtools.2004.04.017

[19] V. Kavimani, K. S. Prakash, T. Thankachan. Influence of machining parameters on wire electrical discharge machining performance of reduced graphene oxide/magnesium composite and its surface integrity characteristics. *Composites Part B: Engineering* **167**:621–630, 2019. https://doi.org/10.1016/j.compositesb.2019.03.031

[20] H. Singh, R. Garg. Effects of process parameters on material removal rate in WEDM manufacturing and processing. *Journal of Achievements in Materials and Manufacturing Engineering* **32**(1):70–74, 2009.

[21] M. E. Asgar, A. K. S. Singholi. Parameter study and optimization of WEDM process: A review. *IOP Conference Series: Materials Science and Engineering* **404**(1):012007, 2018. https://doi.org/10.1088/1757-899X/404/1/012007

[22] L. Urtekin, H. B. Özerkan, C. Cogun, et al. Experimental investigation on wire electric discharge machining of biodegradable AZ91 Mg alloy. *Journal of Materials Engineering and Performance* **30**(10):7752–7761, 2021. https://doi.org/10.1007/s11665-021-05939-2

[23] R. Panwar, N. Sharma, A. Kumar, R. Khanna. Experimental investigation of WEDM control parameters for AZ61 Mg alloy using ANN modeling. *Materials Today: Proceedings* **62**:1397–1401, 2022. https://doi.org/10.1016/j.matpr.2021.12.381

[24] T. U. Siddiqui, J. Ramkumar. Micro-wire electric discharge machining of Mg alloy used in biodegradable orthopaedic implants. *Materials Today: Proceedings* **4**(9):10273–10277, 2017. https://doi.org/10.1016/j.matpr.2017.06.363

[25] N. Ahuja, U. Batra, K. Kumar. Experimental investigation and optimization of wire electrical discharge machining for surface characteristics and corrosion rate of biodegradable Mg alloy. *Journal of Materials Engineering and Performance* **29**(6):4117–4129, 2020. https://doi.org/10.1007/s11665-020-04905-8

[26] M. Somasundaram, J. P. Kumar. Multi response optimization of EDM process parameters for biodegradable AZ31 magnesium alloy using TOPSIS and grey relational analysis. *Sadhana – Academy Proceedings in Engineering Sciences* **47**(3):136, 2022. https://doi.org/10.1007/s12046-022-01908-0

[27] F. Han, J. Jiang, D. Yu. Influence of machining parameters on surface roughness in finish cut of WEDM. *International Journal of Advanced Manufacturing Technology* **34**(5–6):538–546, 2007. https://doi.org/10.1007/s00170-006-0629-9

[28] A. Mostafapor, H. Vahedi. Wire electrical discharge machining of AZ91 magnesium alloy; Investigation of effect of process input parameters on performance characteristics. *Engineering Research Express* **1**(1):015005, 2019. https://doi.org/10.1088/2631-8695/ab26c8

[29] N. Lenin, M. Sivakumar, G. Selvakumar, et al. Optimization of process control parameters for WEDM of Al-LM25/Fly Ash/B4C hybrid composites using evolutionary algorithms: A comparative study. *Metals* **11**(7):1105, 2021. https://doi.org/10.3390/met11071105

[30] D. K. Ammisetti, S. S. H. Kruthiventi. Experimental analysis and artificial neural network teaching – learning-based optimization modeling on electrical discharge machining characteristics of AZ91 composites. *Journal of Materials Engineering and Performance* **33**(21):11718–11735, 2024. https://doi.org/10.1007/s11665-023-08795-4

[31] R. Kumar, P. Katyal, S. Mandhania. Grey relational analysis based multiresponse optimization for WEDM of ZE41A magnesium alloy. *International Journal of Lightweight Materials and Manufacture* **5**(4):543–554, 2022. https://doi.org/10.1016/j.ijlmm.2022.06.003

[32] K. K. Goyal, N. Sharma, R. D. Gupta, et al. Measurement of performance characteristics of WEDM while processing AZ31 Mg-alloy using Levy flight MOGWO for orthopedic application. *International Journal of Advanced Manufacturing Technology* **119**(11–12):7175–7197, 2022. https://doi.org/10.1007/s00170-021-08358-8

[33] A. Muniappan, M. Sriram, C. Thiagarajan, et al. Optimization of WEDM process parameters on machining of AZ91 magnesium alloy using MOORA method. *IOP Conference Series: Materials Science and Engineering* **390**(1):012107, 2018. https://doi.org/10.1088/1757-899X/390/1/012107

[34] S. Gotagunaki, V. S. Mudakappanavar, R. Suresh. Wire electrical discharge machining characteristics of rare earth oxides reinforced AZ91D magnesium alloy hybrid composite using Taguchi-grey relational analysis approach. *Hybrid Advances* **4**:100116, 2023. https://doi.org/10.1016/j.hybadv.2023.100116

[35] S. S. Mahapatra, A. Patnaik. Parametric optimization of wire electrical discharge machining (WEDM) process using Taguchi method. *Journal of the Brazilian Society of Mechanical Sciences and Engineering* **28**(4):422–429, 2006. https://doi.org/10.1590/S1678-58782006000400006

[36] T. Lokeswara Rao, N. Selvaraj. Optimization of WEDM process parameters on titanium alloy using Taguchi method. *International Journal of Modern Engineering Research* **3**(4):2281–2286, 2013.

[37] R. Karthik, R. Viswanathan, J. Balaji, et al. Optimization of WEDM parameters for machining of AZ31B Mg alloy using Taguchi method. *IOP Conference Series: Materials Science and Engineering* **1013**(1):012005, 2021. https://doi.org/10.1088/1757-899X/1013/1/012005

[38] A. Muniappan, R. Solomon, V. Jayakumar, et al. An estimating the effect of control process variables on kerf width in wire EDM of AZ91 magnesium alloy by Taguchi method. *IOP Conference Series: Materials Science and Engineering* **402**(1):012171, 2018. https://doi.org/10.1088/1757-899X/402/1/012171

[39] P. Sivaiah, D. Chakradhar. Modeling and optimization of sustainable manufacturing process in machining of 17-4 PH stainless steel. *Measurement* **134**:142–152, 2019. https://doi.org/10.1016/j.measurement.2018.10.067

[40] A. Ustaoglu, B. Kursuncu, M. Alptekin, M. S. Gok. Performance optimization and parametric evaluation of the cascade vapor compression refrigeration cycle using Taguchi and ANOVA methods. *Applied Thermal Engineering* **180**:115816, 2020. https://doi.org/10.1016/j.applthermaleng.2020.115816

[41] L. Urtekin, F. Yılan, İ. B. Şahin. Optimization of rheology parameters for feedstock by powder injection molding (PIM) via Taguchi analysis. *International Journal of Integrated Engineering* **15**(7):89–101, 2023.

[42] A. Ikram, N. A. Mufti, M. Q. Saleem, A. R. Khan. Parametric optimization for surface roughness, kerf and MRR in wire electrical discharge machining (WEDM) using Taguchi design of experiment. *Journal of Mechanical Science and Technology* **27**(7):2133–2141, 2013. https://doi.org/10.1007/s12206-013-0526-8

[43] U. K. uz Zaman, U. A. Khan, S. Aziz, et al. Optimization of wire electric discharge machining (WEDM) process parameters for AISI 1045 medium carbon steel using Taguchi design of experiments. *Materials* **15**(21):7846, 2022. https://doi.org/10.3390/ma15217846

[44] İ. B. Şahin, F. Yılan, L. Urtekin. Optimisation on machining parametres by EDM of TiN coated Ti6Al4V alloys. *Advances in Materials and Processing Technologies* **10**(2):960–970, 2024. https://doi.org/10.1080/2374068X.2023.2184585

[45] M. A. B. Taher, U. Pelay, S. Russeil, D. Bougeard. A novel design to optimize the optical performances of parabolic trough collector using Taguchi, ANOVA and grey relational analysis methods. *Renewable Energy* **216**:119105, 2023. https://doi.org/10.1016/j.renene.2023.119105

[46] L. Urtekin, İ. B. Şahin, F. Yılan, et al. Investigation and optimization of cutting performance of high chrome white cast iron by wire erosion. *Arabian Journal for Science and Engineering* **49**(2):1585–1596, 2023. https://doi.org/10.1007/s13369-023-07930-6